Layer transfer technique of epitaxial rutile TiO_2 thin films for photonic applications

Sabina Kuprenaite[a], Sylwester Bargiel[a], Pascal Boulet[b], Samuel Margueron[a], Ausrine Bartasyte*[a,c]
[a]FEMTO-ST Institute, University of Franche-Comté, CNRS (UMR 6174), ENSMM, Besançon, France 25030; [c]Jean Lamour Institute, CNRS (UMR 7198), University of Lorraine, Nancy, France 54011; [b]Institut Universitaire de France, Paris, France 75005;

ABSTRACT

Layer transfer technique of epitaxial (00l) oriented rutile TiO_2 films sputtered on sapphire substrates using epitaxial ZnO sacrificial layer was developed. It was demonstrated that obtaining an epitaxial structure for rutile layer transfer can be challenging, due to required control of variety of parameters – surface roughness, growth rate, deposition temperature, interface stresses and lattice matching. It was shown that ZnO, directly grown on M-sapphire substrates, promotes polycrystalline rutile growth. Therefore, 50 nm thick (00l) rutile seed layer with controlled surface roughness grown on M-sapphire substrate was needed to promote the epitaxial $(10\bar{1}3)$ ZnO growth, which then allowed to obtain epitaxial (00l) rutile layer suitable for the layer transfer process. The examined structural quality, evaluated by means of X-ray diffraction and Raman spectroscopy, showed that the transferred rutile films exhibit promising properties for photonic applications.

Keywords: TiO_2 films, rutile, epitaxy, layer transfer

1. INTRODUCTION

TiO_2 films has garnered interest for both its electronic and optical properties[1,2]. Titania can exist in three different crystal structures – rutile (tetragonal, $P4_2/mmm$), anatase (tetragonal, $I4_1/amd$), and brookite (orthorhombic, Pcab). Rutile is the thermodynamically stable TiO_2 phase while anatase and brookite are metastable phases, which can transform to rutile upon heating. While experimental data on brookite is limited due to its rareness and difficult preparation[3], the most used polymorphs are anatase and/or rutile. TiO_2 has an excellent combination of optical properties, that is different for every phase, that make it an advantageous material for several photonic applications, including telecommunications, quantum optics, and photocatalysis[1,4-6]. Rutile and brookite has higher index of refraction (n_e = 2.72 and n_o = 2.67 at 550 nm) than anatase (n_e = 2.60 at 550 nm) and amorphous (n = 2.56 at 550 nm) TiO_2, resulting in better wave confinement and waveguiding properties. Titania also has a wide transparency window spanning the visible and telecom wavelengths (band-edge around 400 nm), a high nonlinear index of refraction, low two-photon absorption, and low fluorescence.[7]

TiO_2 is readily available in the bulk form, however, thin film technology is needed in order to develop scalable photonic devices, as well as it allows to employ the nano- or micro- fabrication lithographic processes, in order to obtain high-precision, scalable, low-footprint, CMOS compatible devices and integrated photonic circuits[1,4,5,7]. TiO_2 films were grown by various deposition methods, such as pulsed laser deposition (PLD)[8], chemical vapor deposition (CVD)[9-10], molecular beam epitaxy (MBE)[11], sol-gel[12] and magnetron sputtering[13-15]. Although amorphous TiO_2 films present lower propagation losses than the polycrystalline anatase and rutile films, the crystalline phases are preferred for their nonlinear properties. To eliminate the propagation losses due to the defective grain boundaries in the polycrystalline films, the epitaxial films have to be considered. Epitaxial growth requires control of various parameters, such as lattice matching with single crystalline substrates, mostly high deposition temperatures, low growth rate, etc. Epitaxial rutile films were grown by PLD on A- and C-sapphire[16], M-sapphire[17], by MBE on R-sapphire[18], by metalorganic CVD on A-sapphire[9] and C-sapphire[10] with the deposition temperatures varying from 450 °C to 800 °C. However, the integrated photonic circuits require the high-quality single-crystal rutile films on the standard SiO_2/Si substrates or other semiconductor platforms. The amorphous SiO_2 does not allow the epitaxial thin film growth and only polycrystalline films can be grown directly. Therefore, direct growth of crystalline TiO_2 films on the integrated photonic platforms remains elusive.

*ausrine.bartasyte@femto-st.fr; phone 33 381402824; https://members.femto-st.fr/ausrine-bartasyte/

In order to obtain epitaxial layers on amorphous layers or substrates with big thermal or lattice mismatches, layer transfer technique can be used. Typically, the layer to be transferred originates from a seed (donor) wafer and is bonded to a recipient wafer and separated from the donor wafer through a thermal or mechanical operation[19]. Layer transfer, using epitaxial lift-off technique has been used to integrate single-crystal GaAs thin films[20]. This technique involves growing the desired thin film on top of a substrate of the same material. A sacrificial layer with high etch-selectivity (e.g. AlAs, ZnO) is deposited between the substrate and thin film to separate the two layers after growth. A black wax (Apiezon W) is used to pick up the thin film and move it to a new substrate. The film is then bonded to the new substrate and the wax is removed. Lattice matching between the substrate and thin film enables high quality epitaxial growth. In addition, this technique enables bonding the thin film to an arbitrary substrate after epitaxial lift-off. Recently very thin epitaxial rutile films (10-70 nm) with mm-scale dimensions were transferred from rutile single-crystal substrates using VO_2 sacrificial layer[21]. However, the wafer-scale compatible TiO_2 layer transfer techniques still need to be developed.

In this paper, layer transfer epitaxial (00l) oriented rutile (offering isotropic optical properties in the substrate plane) from sapphire substrates, available with diameters up to 8 inches, is presented as well, using Au-Au bonding and ZnO as sacrificial and seed layers. The epitaxial films were grown by using magnetron sputtering method, compatible with large scale industrial processing and enabling the epitaxial growth at low temperatures.

2. EXPERIMENTAL DETAILS

TiO_2 films were grown by using radio frequency (RF) magnetron sputtering technique using Ti target (99.99 % purity) in an Ar and 33% O_2 atmosphere with pressure of 5 mTorr. Epitaxial ZnO sacrificial layers were sputtered at a growth rate of 2.8 nm/min. Prior to depositions the M-sapphire substrates (supplied by Roditi) were cleaned in acetone, ethanol and piranha solution (2_{H2SO4}:1_{H2O2}), rinsed with deionised H_2O and blow dried by supressed N_2 gas. The two metal targets of Zn and Ti, were placed in the same sputtering apparatus and the depositions were performed continuously, not exposing deposited films to ambient atmosphere, in order to avoid the possible contamination of each layer, as well as stresses, induced by repeated cooling and heating.

Surface roughness was evaluated by atomic force microscopy (AFM) (Dimension 3100 Veeco). It is important to note that in order to perform the AFM measurements for sacrificial ZnO films, the separate depositions of ZnO/M-sapphire films were done with identical conditions as those for the TiO_2/ZnO/M-sapphire heterostructure. Raman spectra were collected by using an S&I MonoVista Raman spectrometer with laser excitation at 532 nm. The texture and epitaxial quality of grown films were studied by means of X-ray diffraction (XRD). θ/2θ patterns were collected by using a Bruker D8 Advance diffractometer with monochromatic Cu $K_{\alpha 1}$ radiation (1.54056 Å) or AERIS Panalytical diffractometer without monochromator. The rocking curves, φ-scans and pole figures were measured by Bruker D8 Discover diffractometer with Co Kα radiation (1.79026 Å). The lattice strain (ε) was evaluated from the film c-lattice parameter, using equation:

$$\varepsilon_{zz} = \frac{c - c_0}{c_0}, \tag{1}$$

where c_0=2.9592 Å is the bulk rutile TiO_2 c-lattice parameter. The residual stresses (σ) in the film were defined as follows, assuming a biaxial stress in the films:

$$\sigma = \left(C_{13} - \left(\frac{(C_{11} + C_{12}) \times C_{33}}{2 \times C_{13}} \right) \right) \times \varepsilon_{zz}, \tag{2}$$

where the elastic constants C_{ij} in GPa are: C_{11}=271±2; C_{12}=143±0.8; C_{13}=144±2.4 and C_{33}=465±3[22].

Au-Au thermocompression bonding of TiO_2/ZnO/R-sapphire heterostructure with SiO_2/Si substrate was done by using wafer bonder EVG501. 150 nm Au layer with 10 nm Ti adhesion layer were sputtered on both substrates at room temperature, then a uniaxial pressure was applied to bring together the gold films to atomic distance. The bonding process was done at room temperature to avoid thermal stresses.

3. RESULTS

3.1 Epitaxial templates for (00l) rutile films

The possibility to use ZnO as a sacrificial layer was considered, due to its good selectivity of chemical etching and easily tunable epitaxial growth orientation of ZnO films. Initially, epitaxial (00l) rutile growth was expected to be obtained on $(10\bar{1}0)$ ZnO, due to good lattice matching with in plane epitaxial relationship of$(200)_{rutile} \parallel (0006)_{sapph}$ (δ=0.93%) and $(020)_{rutile} \parallel (0002)_{ZnO} \parallel (11\bar{2}0)_{sapph}$ (δ=0.32%), where the lattice mismatch, δ, between ZnO and rutile can be represented by number of unit cell lengths required to match the structures: 10 x $(11\bar{2}0)_{ZnO} \approx$ 7 x $(200)_{rutile}$ and 22x$(0002)_{ZnO} \approx$ 25x$(020)_{rutile}$. For this purpose, 300 nm thick $(10\bar{1}0)$ ZnO was grown on M-sapphire and 150 nm thick rutile was grown on ZnO by magnetron sputtering, both at 350 °C temperature. However, XRD θ/2θ measurements showed that rutile, grown on $(10\bar{1}0)$ ZnO exhibit polycrystalline nature with a minor expected (002) orientation appearance (Figure 1).

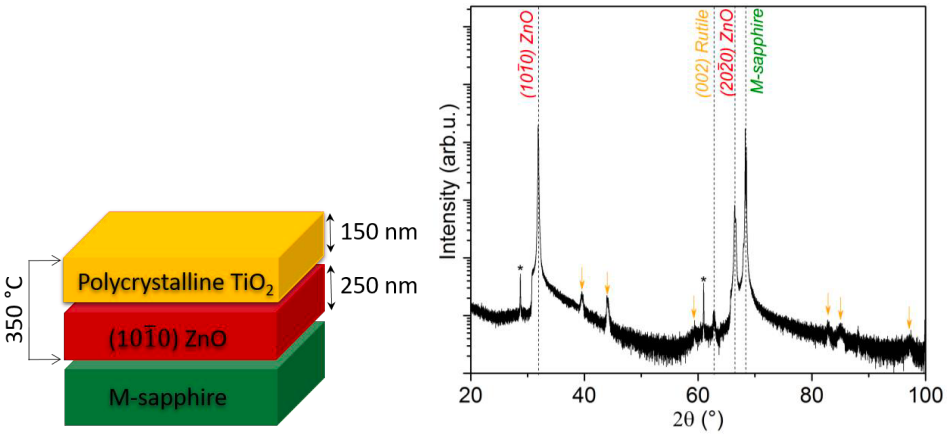

Figure 1. (left) Schematic representation of TiO_2/ZnO/M-sapphire heterostructure; (right) XRD θ/2θ scan of the as-grown heterostructure. The yellow arrows show different observed rutile orientations. *represents K_β reflections from ZnO and sapphire.

To determine the ZnO orientation suitable for epitaxial growth of (00l) rutile, ZnO growth on (00l) rutile layer, epitaxially grown directly on M-sapphire, was tested. It was found that $(10\bar{1}3)$ orientation of ZnO and not $(10\bar{1}0)$ one grows epitaxially on 150 nm thick (002) rutile. The full width at half maximum (FWHM) of $10\bar{1}3$ reflection rocking curve was 0.75° (resolution 0.23°) and FWHM=1.65° of (0002) reflection in φ-scan (resolution 0.45°). The φ scan of (0002) ZnO reflection presented four reflections with $\Delta\varphi = 90°$, indicating four growth domains rotated by 90° in the substrate plane (Figure 2). It can be seen that the (0002) reflections of ZnO are 45° rotated from rutile (111) reflections and match with sapphire $(30\bar{3}0)$ φ-scan reflections. ZnO on rutile/M-sapphire in plane epitaxial relationship can be expressed as: $(10\bar{1}1)'_{ZnO} \parallel (010)_{rutile} \parallel (11\bar{2}0)_{sapph}$ (δ=0.88%) and $(11\bar{2}0)_{ZnO} \parallel (100)_{rutile} \parallel (0006)_{sapph}$ (δ=0.94 %). The $(10\bar{1}1)$ plane is tilted by 3° from the surface plane and therefore it is marked $(10\bar{1}1)'$. Overall, the measurement proves that ZnO film is very well aligned in the plane with respect to epitaxial rutile, grown on M-sapphire.

Therefore, different configurations of rutile/ZnO/M-sapphire heterostructure has been developed, where a thin epitaxial (002) rutile seed layer has been grown directly on M-sapphire, to encourage $(10\bar{1}3)$oriented ZnO epitaxial sacrificial layer growth, which would allow to obtain (002) rutile structural layer. 600°C deposition temperature was chosen in order to obtain the highest epitaxial quality of the grown heterostructure. The schematic representation of the structure can be seen in Figure 3. The 25 nm thick epitaxial (002) rutile was grown on M-sapphire, followed by 300 nm thick ZnO sacrificial layer and 150 nm thick rutile film. The XRD θ/2θ measurement of the as grown heterostructure showed that $(10\bar{1}3)$ oriented ZnO grew with (0002) and $(10\bar{1}0)$ parasitical orientations, what caused (110) and (210) rutile orientations to appear, next to desired (002) (Figure 3).

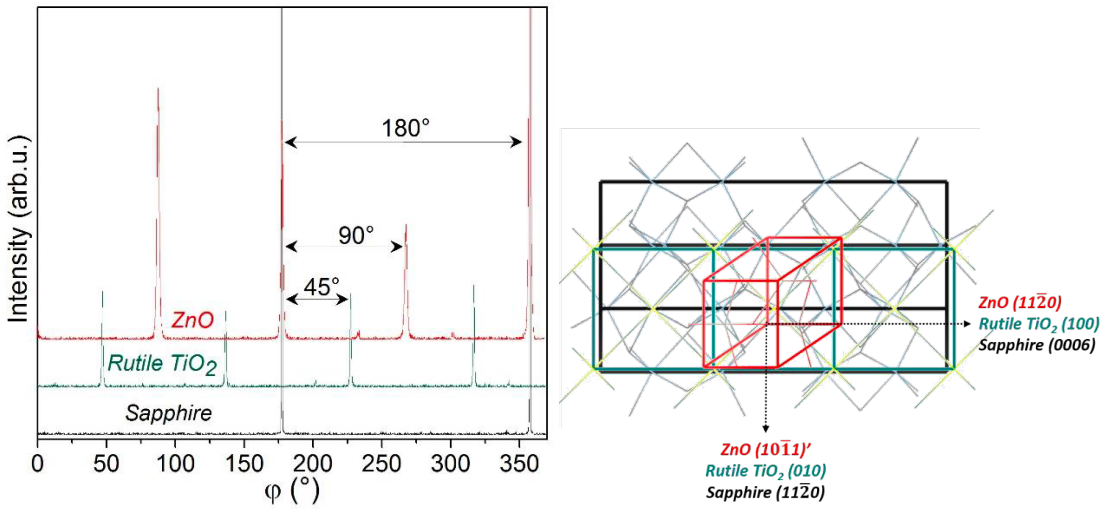

Figure 2. (left) φ-scans of (0002) ZnO plane (measured at χ=31.6°), rutile TiO_2 (111) plane (at χ=42.3°) and sapphire (30$\bar{3}$0) plane (at χ=42.3°). (right) Schematic representation of epitaxial growth of (10$\bar{1}$3) ZnO unit cell (red) on (002) rutile TiO_2 (green) epitaxially grown on (30$\bar{3}$0) sapphire (black).

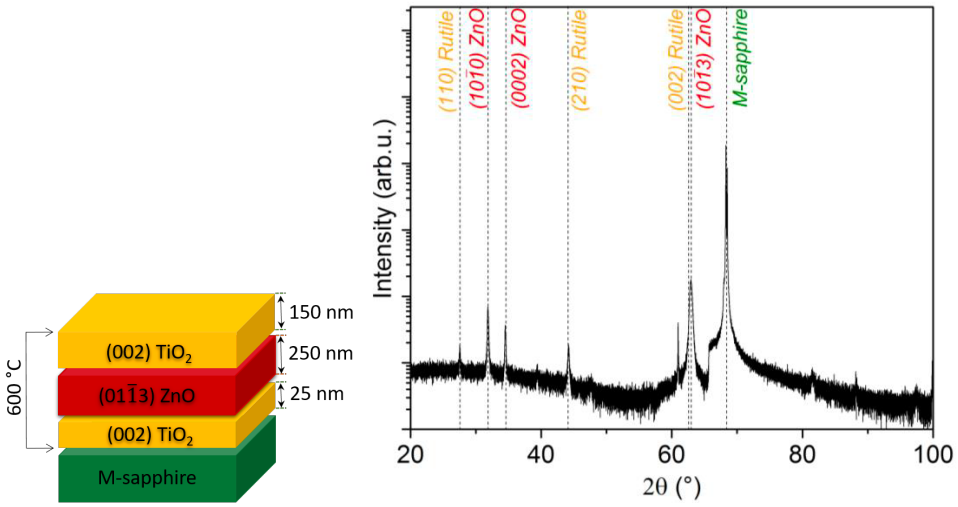

Figure 3. (left) Schematic representation of rutile/ZnO/25 nm rutile/M-sapphire heterostructure; (right) XRD θ/2θ scan of the as-grown heterostructure.

The appearance of additional ZnO orientations with (10$\bar{1}$3) orientation during the growth on 25 m thick (002) rutile film can be explained by analyzing the residual stresses in thin rutile film. The estimation of residual stresses in (002) rutile films on M-sapphire was done from XRD data. A (002) rutile reflection shift towards higher 2θ angles indicated tensile in-plane stress, as the interplanar distance values perpendicular to the substrate plane are reduced. As can be seen in Figure 4, (002) reflection shift (Δ2θ) from the calibrated position of 0.41° was exhibited in the case of 25 nm thick rutile film and the partial relaxation was obtained when the thickness was increased to 50 nm (Δ2θ = 0.06°). The lattice strains (ε_{zz}) were evaluated from the c lattice parameter, using Eq. 1, as well as the residual biaxial stresses (σ) were calculated using the Eq. 2. The results obtained were as follows:

- In the case of 25 nm thick, rutile film $\varepsilon_{zz} = -5.74\times10^{-3}$, $\sigma = 3.0 \pm 0.1$ GPa;
- For 50 nm thick film, $\varepsilon_{zz} = -7.61\times10^{-4}$, $\sigma = 0.4 \pm 0.1$ GPa.

It can be seen that the stresses were reduced almost 10 times, by increasing the film thickness from 25 to 50 nm, therefore it was concluded, that parasitical ZnO orientations were encouraged by distorted rutile lattice parameters and the thicker rutile seed layer could help to obtain pure ($10\bar{1}3$) ZnO epitaxy.

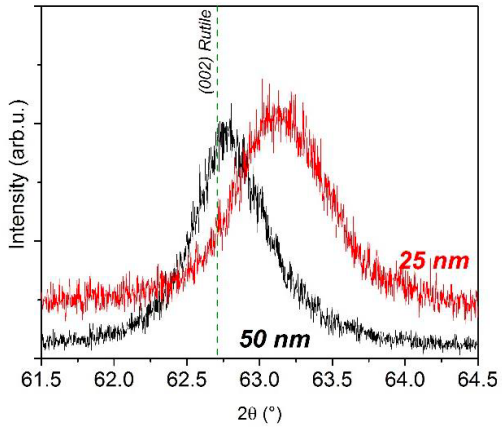

Figure 4. XRD θ/2θ scan of 25 nm and 50 nm thick rutile TiO_2 films grown on M-sapphire at 600 °C deposition temperature. The green dashed line represents the calibrated position of bulk rutile (002) reflection.

Then, the rutile/ZnO/rutile/M-sapphire heterostructure (hereafter 1st structure), with 50 nm thick (002) rutile seed layer, was grown at 600°C (Figure 5). Roughness (Rms) values of the ZnO sacrificial layer and rutile/ZnO/rutile/M-sapphire heterostructure were of 2.65 nm and 6.56 nm, respectively. The XRD θ/2θ measurements showed that the heterostructure exhibited not only desired (002) rutile and ($10\bar{1}3$) ZnO orientations, but also parasitical (110) and (210) rutile orientations were present as well (Figure 6). Thin film surface roughness is an important factor for surface mobility and consequently for epitaxial growth, determining the growth quality of a higher hierarchy layer, and low surface mobility/poor surface quality can cause parasitical orientations to appear. Additionally, bonding and layer transfer processes are very sensitive to film roughness as it can result in poor adhesion between layers. Finally, lower surface roughness is required for low loss propagation. Therefore, in order to reduce the roughness of ZnO and TiO_2 films and to eliminate the parasitical TiO_2 orientations, lower deposition temperature (350 °C) and reduced ZnO growth rate (1.7 nm/min) were used (hereafter 2nd structure, Figure 5). The roughness values of ZnO sacrificial layer and rutile/ZnO/rutile/M-sapphire heterostructure were significantly reduced to 1.68 nm and 2.05 nm, respectively. The XRD θ/2θ scan of the 2nd structure, exhibited only desired (002) rutile and ($10\bar{1}3$) ZnO orientations with no parasitical reflections present in the diffraction pattern (Figure 6).

In order to estimate the texture and epitaxial quality of ZnO and TiO^2 films, XRD rocking curve and φ-scan measurements were performed for the 1st and 2nd grown heterostructures. Similar φ-scan measurement results were obtained for both heterostructures, with 111 rutile reflection FWHM values of 2.17° and 2.43° and (0002) ZnO reflection FWHM values of 1.86° and 2.26°, respectively (±0.45° resolution). Lower FWHM values obtained for the 1st structure can be explained by higher deposition temperature induced higher epitaxial quality, even though parasitical orientations were present in that case and even better epitaxial quality could be obtained in films with pure orientation. The mosaicity was evaluated by performing rocking curve measurements and the FWHM values, obtained for 002 rutile reflection were of 1.16° and 1.95° and for $10\bar{1}3$ ZnO reflection were 1.68° and 1.41°, for the 1st and 2nd structures, respectively. The decrease of rutile rocking curve FWHM value at higher deposition temperature for rutile films is also observed like in case of the φ-scan FWHM value decrease. In the case of the 2nd structure, slightly lower ZnO rocking curve FWHM value could result from lower ZnO growth rate.

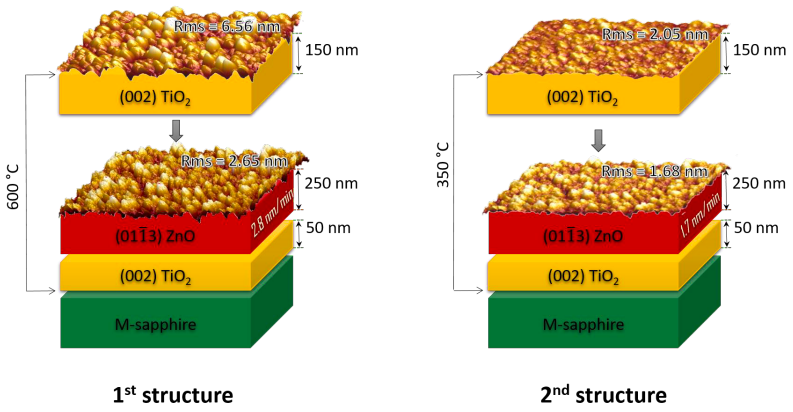

Figure 5. Schematic representation of two rutile/ZnO/rutile heterostructures on M-sapphire substrates: (left) deposition performed at 600 °C, ZnO grown at a rate of 2.8 nm/min; (right) deposition performed at 350 °C, ZnO grown at a rate of 1.7 nm/min. 3D AFM images and estimated roughness values (Rms) are presented on corresponding layers, measured, using the same scale.

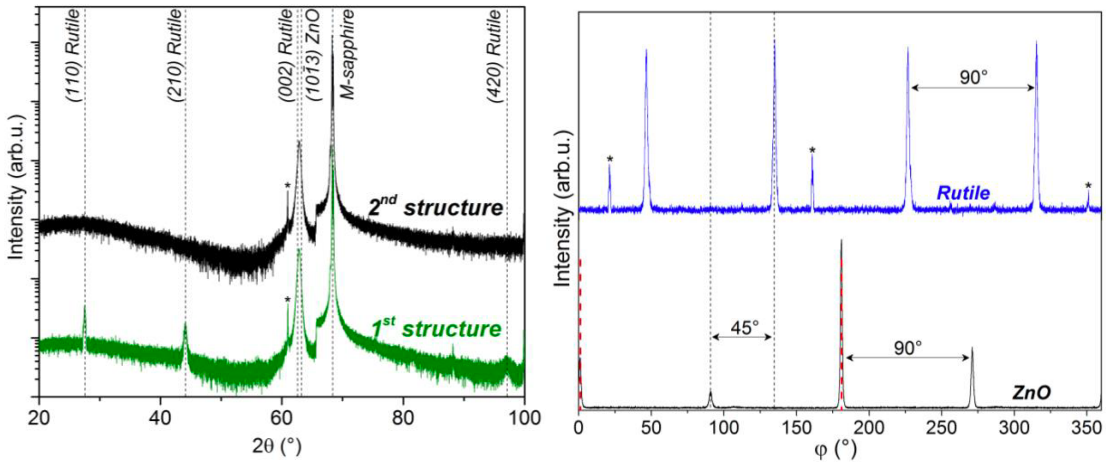

Figure 6. (left) XRD θ/2θ scan of rutile/ZnO/rutile/M-sapphire hererostructures: 1st heterostructure obtained at 600°C (ZnO growth rate 2.8 nm/min) and 2nd one grown at 350°C (ZnO growth rate 1.7 nm/min). (right) φ-scans for (0002) ZnO plane (χ=31.6°) and (111) rutile plane (χ=42.3°). Dashed red lines represent positions of sapphire (30$\bar{3}$0) plane reflections (χ=42.3°). * substrate reflections.

3.2 Rutile layer transfer

The 1st and the 2nd heterostructures were used for the layer transfer process. Although the rutile/ZnO/rutile/M-sapphire heterostructures were optimized on 4-inch wafers. Their Au-Au bonding with SiO_2/Si substrates was performed using 10x12 mm chips, to accelerate the etching of sacrificial layer, thus liberation of "seed" substrate, by using smaller surface area. The schematic representation of the bonding process is given in Figure 7. Series of experiments were performed to estimate the best ZnO etching conditions, however, in order to accelerate the liberation process, 37% HCl acid was chosen. 37% HCl acid was used for ZnO sacrificial layer etching, when the bonded chips were dipped in heated acid and held until the liberation of M-sapphire, with remaining 50 nm thick rutile seed layer, occurs. Even though diluted acid solutions were tested, the series of experiments showed, that the correctly performed bonding procedure was the main factor, determining the success of the liberation process. The XRD θ/2θ measurements were performed for the transferred rutile films, however, no rutile reflections could be seen in the diffraction pattern. It was concluded that due to the bonding process, the film was slightly tilted, and the conventional diffractometer geometry was not suitable to measure the orientation, as the χ angle tilt was needed.

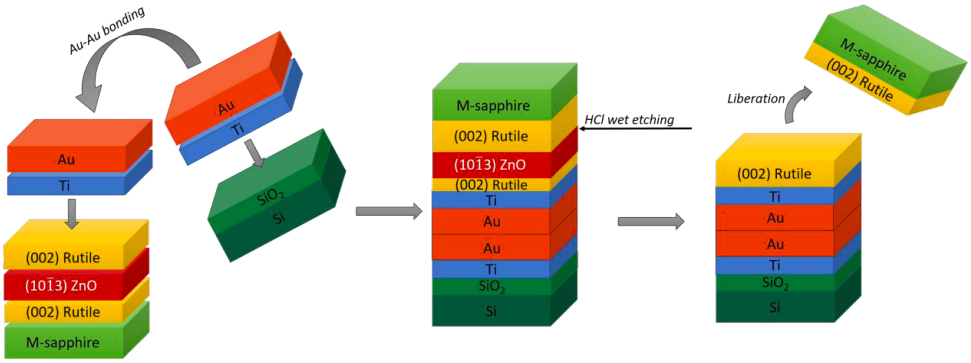

Figure 7. Schematic representation of epitaxial (002) rutile layer transfer on SiO_2/Si substrate, by using sacrificial epitaxial (10$\bar{1}$3) ZnO film and (002) rutile seed layer: (left) growth of rutile/ZnO/rutile/M-sapphire heterostructure and Au-Au bonding to SiO_2/Si substrate, using Ti adhesion layer; (middle) wet etching of ZnO, by using HCl acid; (right) (002) rutile/M-sapphire liberation, obtaining final structure.

Therefore, at the first stage the transferred films were investigated by means of Raman spectroscopy (Figure 8). Three distinctive modes were present at 144 cm^{-1}, 440 cm^{-1} and 612 cm-1, that can be attributed to the rutile phase. The broad band at 235 cm^{-1} has been assigned as the second order mode rather than a fundamental one-phonon process[23]. The B_{1g} mode at 144 cm^{-1} is expected to be very weak in the pure rutile phase[24]. The same Raman spectra was obtained for both, 1st and 2nd transferred structures. To evaluate the texture and epitaxial quality, XRD rocking curve and φ-scan measurements were performed. 4 peaks, separated by 90°, were observed in the φ-scan for (111) rutile plane (Figure 8) like the initial epitaxial templates (Figure 6). The rutile layer, transferred using the 1st heterostructure, presented φ-scan FWHM value of 13.2°, while the layer transferred using the 2nd heterostructure, exhibited 2.5 times smaller φ-scan FWHM value of 5.4°. Even though the epitaxial quality of 1st and 2nd heterostructures before bonding and layer transfer was quite similar, the process and final quality of transferred films was shown to be highly dependent on the surface roughness, which can induce some local curvature and tilting, thus not only reducing the quality, but as well complicating the in-plane XRD measurements. The rocking curve FWHM values were of 0.74° and 0.70°, for the 1st and 2nd heterostructures, respectively, showing quite similar mosaicity and considerably high texture quality. The roughness (RMS) values of transferred rutile layers, obtained by AFM measurements, were of 1.98 and 1.25 nm for the 1st and 2nd structure, respectively.

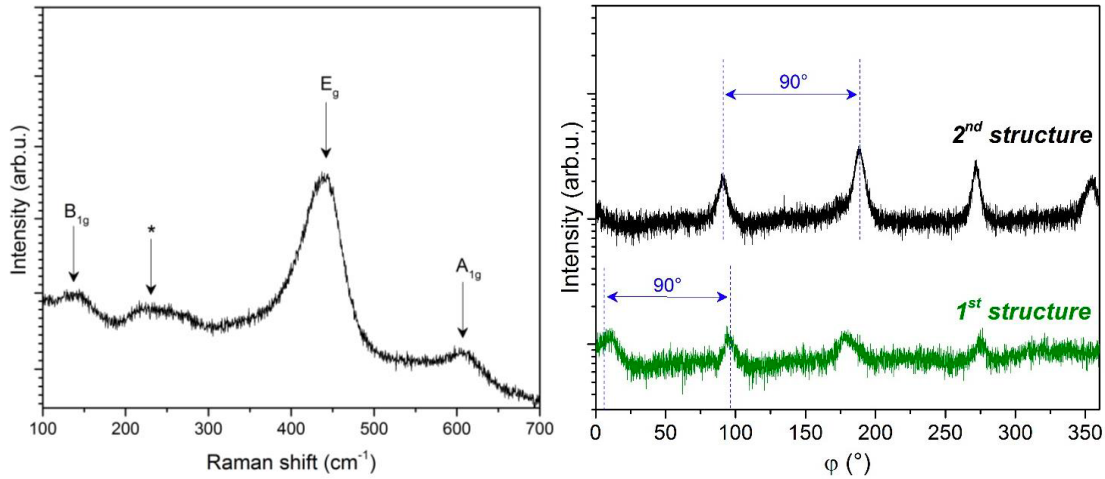

Figure 8. (left) Raman spectra of transferred rutile TiO_2. The band marked with an asterisk is the second order mode. (right) XRD φ-scan measurements for (111) plane (χ=44.4°) of transferred rutile films in the case of 1st and 2nd heterostructures.

4. CONCLUSIONS

Layer transfer technique in this work was applied to transfer (002) epitaxial rutile functional films on SiO_2/Si substrates, by employing Au-Au bonding of chips and sacrificial ZnO layers. It was demonstrated through series of experiments that obtaining an epitaxial structure for layer transferring can be challenging, due to required control of variety of parameters – surface roughness, growth rate, deposition temperature, interface stresses and lattice matching. It was shown that ZnO, directly grown on M-sapphire substrates, promotes polycrystalline rutile growth, even though the calculated lattice matching would suggest that (002) rutile can be grown on $(10\bar{1}0)$ ZnO. Therefore, thin (002) rutile seed layer of 50 nm was directly grown on M-sapphire substrate, to promote the epitaxial $(10\bar{1}3)$ ZnO growth, which then allowed to obtain epitaxial (002) rutile layer to be transferred. The rutile seed layer was shown to exhibit relaxation with thickness, increasing from 25 to 50 nm, therefore inducing better lattice matching with epitaxial $(10\bar{1}3)$ ZnO layer. The roughness of each layer in the heterostructure was shown to be highly important to obtain the top rutile film without any parasitical orientations. It was shown that the lowered growth rate of ZnO, from 2.8 to 1.7 nm/min, can reduce the surface roughness. One of the most important factors for surface roughness control was shown to be deposition temperature, which, reduced from 600°C to 350°C, along with reduced ZnO growth rate, allowed to notably reduce the top rutile layer roughness from 6.56 to 2.05 nm, therefore obtain pure (002) orientation. The transferred rutile film due to bonding imperfections was slightly tilted, therefore no reflections were observed in $\theta/2\theta$ XRD scan, therefore the phase was examined by Raman spectroscopy. The structural quality, evaluated by XRD φ-scan measurements showed that the lower temperature heterostructure presented higher in-plane orientation quality. The examined epitaxial and/or texture quality, evaluated by XRD φ-scan and rocking curve measurements, showed that the transferred films exhibit promising structural properties for photonic applications. To summarize, the presented ability to use sacrificial ZnO layers for rutile functional film layer transferring with desired orientations from sapphire substrates, opens various possibilities for further developments of photonic heterostructures: for example, to use SiO_2 or polymeric bonding, instead of Au-Au one and for up-scaling the process for wafer scale layer transfer.

ACKNOWLEDGEMENTS

This work was supported by the French RENATECH network and its FEMTO-ST technological facility, Bourgogne Franche-Comté region, the French national, and the graduate school EUR EIPHI contract ANR-17-EURE-0002.

REFERENCES

[1] Evans, C.C., et al., “Spectral broadening in anatase titanium dioxide waveguides at telecommunication and near-visible wavelengths”, Opt Express 21(15), 18582-91 (2013).
[2] Strukov, D.B., et al., “The missing memristor found”, Nature 453(7191), 80-3 (2008)
[3] Dambournet, D., Belharouak, I., and Amine, K., “Tailored Preparation Methods of TiO_2 Anatase, Rutile, Brookite: Mechanism of Formation and Electrochemical Properties”, Chemistry of Materials 22(3), 1173-1179 (2010).
[4] Reshef, O., et al., “Polycrystalline anatase titanium dioxide microring resonators with negative thermo-optic coefficient” Journal of the Optical Society of America B 32(11) (2015).
[5] Borne, A., Segonds, P., Felix, C., Debray, J., “Refractive indices, phase-matching directions and third order nonlinear coefficients of rutile TiO_2 from third harmonic generation”, Optical Materials Express 2(12), 1797-1802 (2012).
[6] Ohno, T., Sarukawa, K., and Matsumura, M., “Crystal faces of rutile and anatase TiO_2 particles and their roles in photocatalytic reactions”, New Journal of Chemistry 26(9), 1167-1170 (2002).
[7] Evans, C.C., Bradley, J.D.B., Marti-Panameno, E.A., Mazur, E., “Mixed two- and three-photon absorption in bulk rutile (TiO2) around 800 nm”, Optics Express 20(3), 3118-3128 (2012).
[8] Kitazawa, S.-I., et al., “Rutile and anatase mixed crystal TiO_2 thin films prepared by pulsed laser deposition”, Thin Solid Films 515(4), 1901-1904 (2006).

[9] Chang, H.L.M., You, H., Gao, Y., Guo, J., Foster, C.M., Chiarello, R.P., Zhang, T.J., Lam, D.J., "Structural properties of epitaxial TiO_2 films grown on sapphire (11-20) by MOCVD", Journal of Materials Research 7(9), 2495-2506 (1992).
[10] Chang, H.L.M., Zhang, T.J., Zhang, H., Guo, J., Kim, H.K., Lam, D.J., "Epitaxy, microstructure, and processing-structure relationships of TiO_2 thin films grown on sapphire (0001) by MOCVD", Journal of Materials Research 8(10), 2634-2643 (1993).
[11] Murakami, M., et al., "Anatase TiO_2 thin films grown on lattice-matched $LaAlO_3$ substrate by laser molecular-beam epitaxy", Applied Physics Letters 78(18), 2664-2666 (2001).
[12] Gratzel, M., "Sol-Gel Processed TiO_2 Films for Photovoltaic Applications", Journal of Sol-Gel Science and Technology 22, 7-13 (2001).
[13] Heo, C.H., Lee, S.-B., and Boo, J.-H., "Deposition of TiO_2 thin films using RF magnetron sputtering method and study of their surface characteristics", Thin Solid Films 475(1-2), 183-188 (2005).
[14] Tanemura, S., et al., "Optical properties of polycrystalline and epitaxial anatase and rutile TiO_2 thin films by rf magnetron sputtering" Applied Surface Science 212-213, 654-660 (2003).
[15] Tanemura, S., Miao, L., Wunderlich, W., Tanemura, M., Mori, Y., Toh, S., Kaneko, K., "Fabrication and characterisation of anatase/rutile-TiO_2 thin films by magnetron sputtering: a review" Science and Technology of Advanced Materials 6(1), 11-17 (2005).
[16] Sbaï, N., et al., "Epitaxial growth of titanium oxide thin films on c-cut and α-cut sapphire substrates", Surface Science 601(23), 5649-5658 (2007).
[17] Bayati, M.R., et al., "Structure–property correlation in epitaxial (200) rutile films on sapphire substrates", Journal of Solid State Chemistry 187, 231-237 (2012).
[18] Engel-Herbert, R., et al., "Microstructure of epitaxial rutile TiO_2 films grown by molecular beam epitaxy on r-plane Al_2O_3" Journal of Crystal Growth 312(1), 149-153 (2009).
[19] Rogers, D. J., et al., "Novel process for direct bonding of GaN onto glass substrates using sacrificial ZnO template layers to chemically lift-off GaN from c-sapphire", Proc. SPIE 8263, Oxide-based Materials and Devices III, 82630R
[20] Demeester, I.P., De Dobbelaere, P., Brys, C., Van Daele, P., "Epitaxial lift-off and its applications", Semicond. Sci. Technol. 8, 1124-1135 (1993).
[21] Lee, D.K., Park, Y., Sim, H. et al. "Heterogeneous integration of single-crystalline rutile nanomembranes with steep phase transition on silicon substrates", Nat. Commun. 12, 5019 (2021).
[22] Mahmood, T., et al., "Electronic, elastic, optical properties of rutile TiO_2 under pressure: A DFT study", Physica B: Condensed Matter 407(6), 958-965 (2012).
[23] Porto, S.P.S., Fleury, P.A., and Damen, T.C., "Raman Spectra of TiO_2, MgF_2, ZnF_2, FeF_2, and MnF_2", Physical Review 154(2), 522-526 (1967).
[24] Suryanarayanan, R., et al., "Room temperature ferromagnetism in spin-coated anatase- and rutile-$Ti_{0.95}Fe_{0.05}O_2$ films", Journal of Physics: Condensed Matter 17(4), 755-762 (2005).